# *LEG 180*
# *Woodlark Basin*

# LEG 180

## ACTIVE CONTINENTAL EXTENSION IN THE WESTERN WOODLARK BASIN

**Modified by B. Taylor From Proposal 447-Rev3 Submitted By:**

**B. Taylor, J. Mutter, F. Martinez, A. Goodliffe, G. Abers, C. Mutter, R. Binns, H. Davies, and S. Scott**

**Staff Scientist: Adam Klaus** **Co-Chief Scientists: Brian Taylor, Philippe Huchon**

### ABSTRACT

The lateral variation from active continental rifting to seafloor spreading within a small region makes the western Woodlark Basin an attractive area to investigate the mechanics of lithospheric extension. Earthquake source parameters and seismic reflection data indicate that low-angle (~25°) normal faulting is active in the region of incipient continental separation. A low-angle normal fault emerges along the northern flank of Moresby Seamount, a continental crustal block with green-schist metamorphic basement. Asymmetric basement fault blocks overlain by only minor ponded sediments characterize the margin to the south, whereas the margin to the north has a down-flexed pre-rift sedimentary basin and basement sequence unconformably onlapped by synrift sediments.

Leg 180 will drill a transect of sites just ahead of the spreading tip: ACE-1c and ACE-7b on the down-flexed northern margin; ACE-8a through the rift basin sediments, the low-angle normal fault zone, and into the footwall; and ACE-3c near the crest of Moresby Seamount.

The primary objectives at these sites are to: (1) characterize the in situ properties (stress, permeability, temperature, pressure, physical properties, fluid pressure) of an active low-angle normal fault zone to understand how such faults slip, and (2) determine the vertical motion history of both the down-flexed hanging wall and the unloaded footwall and, thereby, derive the timing and amount of extension prior to spreading initiation.

## INTRODUCTION

The processes by which continental lithosphere accommodates strain during rifting and the initiation of seafloor spreading are presently known primarily from the study of either (1) passive margins bordering rifted continents, where extensional tectonics have long ceased and evidence for active tectonic processes must be reconstructed from a record that is deeply buried in post-rift sediments and thermally equilibrated, or (2) regions of intracontinental extension, such as the U.S. Basin and Range and the Aegean, where extension has occurred recently by comparison to most passive margin examples, but has not proceeded to the point of continental breakup.

One particularly controversial conjecture from these studies is that aerially large normal detachment faults dip at low angles and accommodate very large amounts of strain through simple shear of the entire lithosphere. The role of low-angle normal detachment faults has been contested strongly, both on observational and theoretical grounds. It has been suggested that intra-continental detachments have been misinterpreted and actually formed by roll-over of originally high-angle features, or that they occur at the brittle-ductile boundary in a pure shear system. Theoretically, it has been shown that normal faulting on detachment surfaces would require that the fault be extremely weak—almost frictionless—to allow horizontal stresses to cause failure on low-angle planes. The growing evidence for a weak fault and strong crust associated with motion on the San Andreas transform fault supports the weak normal detachment fault model, and models abound in the literature in which low-angle detachment faulting is an essential mechanism of large-scale strain accommodation.

Nevertheless, the mechanisms by which friction might be effectively reduced on low-angle normal fault surfaces are not understood. One possibility is that active shearing in the fault zone creates a strong permeability contrast with the surrounding crust (by opening cracks more quickly than precipitation can heal them), allowing pore-pressure distributions that are high and near to the fault-normal compressive stress within the fault zone, but that decrease with distance into the adjacent crust (Rice, 1992; Axen, 1992). Testing for such fault-proximal high permeability and pore pressures and the associated local rotation of stress axes requires drilling into an active system.

This would also allow determination of the properties of the fault rock at depth (do they exhibit reduced frictional strength at higher slip velocities, consistent with unstable sliding and observed earthquakes?) as well as studies of the mechanisms by which fluid-rock reactions affect deformation (constitutive response, frictional stability, long-term fault strength)—see Hickman et al. (1993) and Barton et al. (1995) for extensive discussion of the mechanical involvement of fluids in faulting, and Wernicke (1995) for a review of low-angle normal faulting.

The continuum of active extensional processes, laterally varying from continental rifting to seafloor spreading in the western Woodlark Basin-Papuan Peninsula region of Papua New Guinea (Fig. 1) provides the opportunity to test these various models. Seafloor spreading magnetic anomalies indicate that during the last 6 m.y. the formerly contiguous, eastward extensions of the Papuan Peninsula (the Woodlark and Pocklington rises) were separated as a westward propagating spreading center opened the Woodlark Basin about a pole close to Port Moresby (~9.5°S, 147°E). The current spreading tip is at 9.8°S, 151.7°E. Farther west, extension is accommodated by continental rifting, with associated full and half graben, metamorphic core complexes and peralkaline rhyolitic volcanism. Earthquake source parameters and seismic reflection data indicate that low-angle normal faulting is active in the region of incipient continental separation (Figs. 2-5; Abers, 1991; Taylor et al., 1995, 1996; Mutter et al., 1996; Abers et al., in press). Leg 180 will drill a transect of sites (just ahead of the spreading tip) above, below, and through a low-angle normal fault to determine the vertical motion and horizontal extension history prior to seafloor spreading, and to characterize the in situ properties of the active fault zone.

## BACKGROUND

### Recent Research Programs

Several recent research programs have significantly improved our understanding of the regional geological and geophysical setting of rifting into the Papuan Peninsula (Figs. 1-3):

1. Sidescan and underway geophysical surveys have provided bathymetry, acoustic imagery,

magnetization, and gravity maps, and allowed detailed reconstructions of the spreading history (Taylor et al., 1995, 1996; Goodliffe et al., 1997, and A. Goodliffe, unpublished data).

2. Multichannel seismic reflection surveys reveal the upper crustal architecture of the rifting region, including the presence of low-angle normal faults (Figs. 3-5; Mutter et al., 1996; Taylor et al., 1996).

3. The PACLARK and SUPACLARK series of cruises in 1986-1991 (Binns, Scott et al., 1987, 1989, 1990; Lisitsin et al., 1991; Benes et al., 1994) included dredging, coring, camera and video observations, and seven *Mir* submersible dives. The bottom samples include Normal Mid-Ocean Ridge Basalt (N-MORB) from the youngest spreading segments, as well as greenschist facies metamorphics from the lower north flank of Moresby Seamount. In contrast, a 1995 site survey dredged late Pliocene (synrift) sedimentary rocks from the upper south flank of Moresby Seamount—apparently precluding a metamorphic core complex origin for this feature (Taylor et al., 1996).

4. Abers (1991) and Abers et al. (in press) determined source parameters and relocated earthquakes in the rifting region. The focal mechanisms are all extensional or strike-slip with northerly tension axes (T-axes; Fig. 2). Several are consistent with slip on shallow-dipping normal faults.

5. Studies of metamorphic core complexes on the Papuan Peninsula, D'Entrecasteaux and Misima Islands, show that (a) they are associated with Pliocene-Pleistocene granodiorite intrusions and amphibolite-facies ductile shear zones, (b) they have been rapidly exhumed from ~30 km depth (7-11 kilobar [kb]) in 4 m.y., (c) uplift continues (forming topography up to 2.5 km), and (d) they are very three dimensional and regionally discontinuous (or varying in grade) along strike (Davies and Warren, 1988, 1992; Hill, 1987, 1990, 1994, 1995; Hill et al., 1992, 1995; Hill and Baldwin, 1993; Baldwin et al., 1993; Lister and Baldwin, 1993; Baldwin and Ireland, 1995).

6. The Papuan Ultramafic Belt is a late Paleocene to early Eocene supra-subduction zone ophiolite

with gabbros and boninites $^{40}Ar/^{39}Ar$ dated at 59 Ma (R. Duncan, pers. comm. 1993; Walker and McDougall, 1982), P4 (late Paleocene) foram-bearing micrites overlying the basalts, with tonalite-diorite-dacite intrusions K/Ar dated at 57-47 Ma (Rogerson et al., 1993). This revision to dating of the Papuan Peninsula basement allows a simplified geological evolution for the region, as outlined below.

## Papuan Crustal Evolution

### *Paleogene Subduction and Collision*

Much of the Papuan Peninsula is 1-3 km above sea level and is underlain by crust 25-50 km thick (Finlayson et al., 1976). Major orogenic thickening of the crust occurred following the northeast subduction and partial accretion of a thick sequence of dominantly Cretaceous to Eocene strata beneath a late Paleocene-early Eocene island arc that includes the Papuan Ultramafic Belt (PUB), Milne Basic Complex, and Cape Vogel boninites (Davies and Jaques, 1984; Davies et al., 1984; Rogerson et al., 1987, 1993). Collision of the Australian (Papuan) continental margin plateau caused subduction to cease and uplifted the accretionary complex (Owen Stanley Metamorphics) by the early Miocene (Rogerson et al., 1987). Metabasites in the Emo metamorphics and Suckling-Dayman massif (the latter with a cover of Maastrichtian micrites) have been exhumed from 7-12 kb (25-35 km) and may represent slivers of the subducted Cretaceous oceanic crust (Davies, 1980; Worthing, 1988).

The pre-Miocene geology of the islands on the Pocklington and Woodlark Rises is similar to that of the Papuan Peninsula, with Owen Stanley Metamorphics in the south (Misima, Tagula, and Rossel Islands) and Milne Basic Complex outcrops on Woodlark Island (Davies and Smith, 1971; Ashley and Flood, 1981). Likewise, late Paleocene volcanics occur at the base of the Nubiam 1 well (Stewart et al., 1986), west of the Trobriand Islands, and the metamorphic core complexes on the D'Entrecasteaux Islands have a core of Owen Stanley Metamorphics and a cover of unmetamorphosed PUB ultramafics (Davies and Warren, 1988).

### *Miocene-Quaternary Arc and Forearc*

Superimposed on this Paleogene basement is widespread middle Miocene to Holocene calc-alkaline and shoshonitic magmatism (Smith and Milsom, 1984) associated with southwest subduction of the Solomon Sea Basin at the Trobriand Trough. Active arc volcanism and a deforming accretionary prism are compatible with present-day slow subduction at the Trobriand Trough (Hamilton, 1979; Davies and Jaques, 1984; Lock et al., 1987), though this remains controversial given the small number of intermediate-depth earthquakes beneath the region (Abers and Roecker, 1991) and the lack of $^{10}$Be in the arc lavas (Gill et al., 1993). The geochemistry of the volcanics reveals melting and mixing of at least three magma sources: (1) subduction-modified mantle supplied the calc-alkaline arc volcanism; (2) this mantle, with the addition of partial melts from upwelling aesthenosphere, produced the comenditic (transitional basalt-peralkaline rhyolites) series around Dawson Strait; and (3) contamination by lower crust of Australian affinity formed minor high-K trachytes (see Smith, 1976; Hegner and Smith, 1992; Stolz et al., 1993; and references therein).

The Cape Vogel (including Trobriand) Basin is a Neogene forearc basin, characterized by middle Miocene subsidence, volcanism, deep marine sedimentation, late Miocene uplift and erosion (1-2 km) of the margins, and Pliocene coarse clastic (from uplift of the Papuan Peninsula and D'Entrecasteaux Islands to the south) and Quaternary carbonate, shallow-water sedimentation during broad subsidence (Tjhin, 1976; Stewart et al., 1986; Francis, 1987; Davies and Warren, 1988). The basin experienced late Miocene/Pliocene inversion in the northwest, but its center continues to subside in the southeast (Pinchin and Bembrick, 1985). The Lusancay-Trobriand-Woodlark Islands sit atop an outer forearc structural high with an associated 150-200 mgal free-air gravity anomaly.

The Trobriand Trough, the outer forearc structural and gravity high, and the Cape Vogel forearc basin terminate near Woodlark Island. Farther east, the Woodlark and Pocklington rises were not a Plio-Pleistocene arc-forearc system. Rather, the northern edge of the eastern Woodlark Rise was a transform margin, and seismicity and sidescan data indicate that it is still an active right-lateral fault. Thus, the Woodlark Basin did not originate as a backarc basin, in that the eastern Woodlark and Pocklington rises were not active island arcs (Weissel et al., 1982). Nevertheless, the locus of present rifting (see below) bisects an inherited crustal asymmetry, with the Neogene forearc basin to the north and the Paleogene accretionary/collision complex and Neogene backarc to the south.

### *Plio-Pleistocene Rifting*

Shallow seismicity, with extensional and strike-slip focal mechanisms having northerly T-axes, is concentrated east of the D'Entrecasteaux Islands and extends westward into the Papuan Peninsula at 9°-10°S to about 148°E (Fig. 2; Weissel et al., 1982; Abers, 1991; Abers et al., in press). Plio-Pleistocene extension has produced three flooded grabens (Mullins Harbor, Milne Bay and Goodenough Bay) on the eastern extremity of the Papuan Peninsula with associated rift-flank subaerial uplift to over 500 m (Smith and Simpson, 1972). Metamorphic core complexes on the D'Entrecasteaux Islands and in the Suckling-Dayman massif on the Papuan Peninsula were also exhumed in the Plio-Pleistocene (Davies, 1980; Davies and Warren, 1988; Hill, 1990). The best structural studies, geothermometry, geobarometry, and age dating of these complexes have been done on Goodenough and Furgusson Islands (Davies and Warren, 1992; Hill et al., 1992, 1995; Hill and Baldwin, 1993; Baldwin et al., 1993; Lister and Baldwin, 1993; Hill, 1994; Baldwin and Ireland, 1995). There, normal movement along a 0.3 to 1.5-km-thick ductile mylonitic shear zone resulted in the uplift of deep metamorphic rocks and the juxtaposition of unmetamorphosed cover rocks. Granodioritic intrusion then focused uplift on several domes, offset by strike-slip faults. The ductile shear zones were brecciated and truncated by brittle faults late in their history. These domal structures are juxtaposed along strike with regions of significantly less unroofing, such as the low (greenschist) grade eastern halves of both Normanby and Misima islands.

## **Woodlark Basin Evolution**

The oldest magnetic anomalies (An.3R), in the extreme east of the basin, indicate seafloor spreading began by 6 Ma (Taylor, 1987; Taylor and Exon, 1987). Spreading has sequentially transgressed westward, stepping across Moresby Transform (154.2°E) about 2 Ma (just prior to An.2) to reach its current tip at 151.7°E (Figs. 1, 2). Bruhnes Chron spreading rates decrease from 67 mm/yr at 156.2°E to 36 mm/yr at 152°E (Fig. 1).

The sidescan and geophysical data show that the rifting-to-spreading transition involves both nucleation of discrete spreading cells and organized ridge propagation (Taylor et al., 1995). Two ridge propagation events into the margin at 153°E formed continental slivers surrounded by oceanic crust. Spreading is about to propagate into this margin again. Rifting of the conjugate margins continues for ~1 m.y. after spreading has separated them. Extension does not immediately localize to the ridge axis, as shown by the present overlap between spreading and seismogenic margin faulting, and by inwardly curved seafloor fabric and magnetic anomalies that require nonrigid margin reconstructions. The initial spreading system lacks transform faults and has both overlapping and orthogonally offset segments (Figs. 1, 2). The 50-km-offset Moresby Transform Fault formed by cutting through rifted crust to join overlapping spreading segments of initial oceanic crust. It is not contiguous with transfer faults in the rifted margins. The initial spreading system evolves by ridge propagation, transform development, and ridge jumping/rotation.

Seismic reflection data indicate a very sharp (1 to 2 km wide at the surface) transition from rifted crust to oceanic crust. There are no dipping reflector sequences indicative of excessive lava production and high degrees of mantle partial melting, but there are small volcanoes a few kilometers in diameter that are often erupted along margin faults. Indeed, the initial seafloor spreading lavas indicate low degrees of partial melting:  basalts from the youngest spreading segment, just east of Moresby Seamount, have $Na_8$ = 3.1 (Binns and Whitford, 1987). Other young axial lavas include FeTi basalts, and low- and high-Si andesites with evidence for both mantle heterogeneity and crustal contamination.

**Drilling Area**

The rifting region just ahead of the apex of spreading has been imaged by several seismic reflection surveys (Figs. 3-5; Mutter et al., 1993, 1996; Goodliffe et al., 1993; Taylor et al., 1996). North of Moresby Seamount, a low-angle normal fault dips north beneath a down-flexed pre-rift sedimentary basin and basement sequence, unconformably onlapped by synrift sediments that are cut by higher angle normal faults with a zig-zag pattern in plan view (Figs. 2-5). The seismic stratigraphy can be reasonably jump-correlated to that in the Trobriand Basin and is interpreted to be a Pliocene to Quaternary synrift sequence lying unconformably above a Miocene forearc basin sequence on Paleogene volcanic and metamorphic basement (Fig. 5). To the south of Moresby Seamount, high-relief rotated fault blocks are commonly overlain by only minor ponded sediments.

Shallow (2-10 km) normal and strike slip faults, with northerly T-axes, bound the north side of the rifting-spreading transition (Fig. 2; Abers, 1991; Taylor et al., 1995; Abers et al., in press). All of the earthquake hypocenters occur within or north of the rift graben, and there are no major extensional structures north of the graben-bounding antithetic fault. Without local seismometers, the teleseismicity can not be definitively associated with the low-angle reflector, but there is no more likely candidate structure. Furthermore, the seismic stratigraphy of the profiles in Figure 3 can not be matched without recent faulting on the low-angle reflector.

Two dredges of the northern flank of Moresby Seamount recovered metabasic greenschists, metagabbro, pelitic schist, and minor siliceous phyllite and microgranite; i.e., similar material to the low-grade (greenschist) metamorphics on eastern Normanby and Misima Islands, not the core complex amphibolite metamorphics on Goodenough, Fergusson, and NW Normanby (H. Craig, 1986, unpublished SIO cruise report; Binns et al., 1987; J. Hill, pers. comm., 1996). In contrast, a dredge from 541 to 1211 m (~0.7-1.6 s two way traveltime [TWT]) on the upper southern flank of the seamount recovered late Pliocene (N21 = 1.9-3.1 Ma) clastic sedimentary rocks of equivalent facies to the Awaitapu Formation of the Trobriand region in the Cape Vogel Basin (Francis et al., 1987). Benthic foraminifers indicate sediment deposition in water depths of 340-800 m (J. Resig, pers. comm., 1995). These rocks are equivalent to those that we infer lie near the base of the synrift cover sequence in the rift basin and on the northern margin.

A cross section consistent with the available seismic and dredge data is drawn in Figure 5 (Taylor et al., 1996). At the end of the Miocene, the Paleogene basement and a forearc basin filled with Miocene sediment were being eroded at or near sea level. Pliocene rifting formed sediment-filled grabens in the southern orogenically thickened arc province, accompanied by gradual subsidence of the thinner, colder (and therefore stronger) forearc to the north (inferred Pliocene sediments are dotted in Fig. 5). Quaternary stretching localized on a low-angle normal fault (the antithetic hanging-wall fault accommodated little additional extension). The northern margin flexed down southward and was onlapped by sediments delivered via submarine channels incising northward. Recently, continued extension on the low-angle fault variably collapsed the hanging-wall graben, into which sediments are now prograding from the north.

This interpretation predicts about 12 km of heave on the low-angle fault. This compares with at least 130 km of total extension in the 4 m.y. prior to spreading at this longitude, calculated from the pole of opening derived from seafloor spreading magnetic anomalies, and probably greater amounts back to the beginning of spreading at >6 Ma (Taylor et al., 1996). Given only minor extension of the northern, flexed margin, we infer that the locus of current extension must be the northernmost of a series of similar structures that extended weak crust to the south, forming the block-faulted Pocklington Rise. The regional estimates predict that this rugged province of mainly inactive faults accommodated >120 km of total strain as it collapsed from heights comparable to the 3-km-high Owen Stanley Ranges that form the backbone of the Papuan Peninsula. We do not know where to locate so much extension given a current total width of 200 km for this province.

## SCIENTIFIC OBJECTIVES

The western Woodlark Basin is arguably the best characterized region of active continental breakup. The proximity of a seismogenic low-angle normal fault that has been imaged by seismic reflection data and zero-offset conjugate margins that are about to be penetrated by seafloor spreading is unique. There are two major objectives for drilling in this region. Both are within the broader context of understanding the physical processes and mechanics of lithospheric extension:

1. Characterize the in situ properties (stress, permeability, temperature, pressure, physical properties, and fluid pressure) of an active low-angle normal-fault zone to understand how such faults slip. Questions to be answered include the following: What are the differences in

properties of the active fault compared to the surrounding crust? How is friction effectively reduced? Is there a strong permeability and fluid pressure contrast between the fault zone and its surroundings? Do the fault zone materials exhibit reduced frictional strength at higher slip velocities, consistent with unstable sliding? How do fluid-rock reactions affect the deformation mechanisms?

2. Determine the vertical motion history of both the down-flexed hanging wall and the unloaded footwall (by backstripping the biostratigraphy, regionalizing the well data using seismic stratigraphy, and by Pressure-Temperature-time [P-T-t] data and petrofabric studies of metamorphic basement), and thereby deriving the timing and amount of extension prior to spreading initiation (for which different local vs. regional estimates exist).

Drilling a very deep hole (>2.5 km) through the low-angle normal fault in the seismogenic zone, where both the footwall and hanging wall are composed of basement, remains our long-term objective. However, as Leg 180 will penetrate only ~1200 m across the fault zone, this and further fault zone experiments and monitoring (e.g., CORK) will require a future leg.

## DRILLING STRATEGY

Leg 180 will drill a transect composed of sites across an asymmetric incipient conjugate margin pair (a few miles ahead of the spreading tip): Sites ACE-1c and ACE-7b on the down-flexed northern margin; Site ACE-8a through the rift basin sediments, the active low-angle normal fault zone, and into the footwall; and Site ACE-3c near the crest of the footwall fault block (Moresby Seamount). Water depths at the drill sites range from 420 m to 3180 m.

The four sites are located within a grid of multichannel seismic (MCS) lines and multibeam bathymetry (Fig. 3), and each will involve an advanced hydraulic piston corer/extended core barrel (APC/XCB) hole followed by a rotary core barrel (RCB) hole. The northern sites are designed to penetrate the Pliocene-Quaternary hemipelagic cover sequence into the pre-rift section: Miocene forearc clastics at Site ACE-7b and Paleogene basement at Site ACE-1c. A free-fall funnel will likely be needed to achieve 200 m penetration into greenschist facies metamorphic basement beneath the 300-m-thick Pliocene-Quaternary section at Site ACE-3c.

Proposed Sites ACE-1c and ACE-3c will be drilled before the triple casing rentry hole at Site ACE-8a to provide initial characterization of the Quaternary rift fill and the basement expected there. Casing is needed in anticipation of possibly unstable sediments (resulting from rapid deposition and faulting), an active fault zone (probably overpressured), and anisotropic basement (probably sheared and altered). Operations will have to run smoothly in order to have time to complete Site ACE-7b.

## LOGGING PLAN

All sites will be logged with the Triple-combo, Formation MicroScanner (FMS), and Geological High-resolution Magnetometer (GHMT) tools. The Triple-combo will provide temperature, geophysical, and physical property data and is the basis for core-log integration. The Azimuthal Resistivity Imager (ARI) will be used to measure resistivity (and resistivity anisotropy) in igneous environments. Geochemical logs will contribute to complete basement identification. Standard logs also provide a means to compute synthetic seismograms, hence linking borehole data to large-scale MCS profiles. The FMS images will provide structural fabric data, a means to orient core, and stress-related hole ellipticity. The GHMT will locate magnetic reversals and aid core-log integration via magnetic susceptibility.

The BoreHole TeleViewer will be run in basement at Sites ACE-1c, 3a, and 8a to ultrasonically image lithostratigraphy, fracture orientation, and the nature of stress-induced borehole breakouts—from which the direction of horizontal stresses may be deduced. In addition, at the site (ACE-8a) of inferred active faulting, modeling of the observed interactions between breakouts and fractures may be used to obtain information about the magnitude of in situ stress (Barton and Zoback, 1994).

At Site ACE-8a, each successive casing string will be added after downhole measurements of the previously drilled section. The Schlumberger 5-element array seismic imager (ASI) will be used for a vertical seismic profile to accurately tie the well to the MCS data. A drill-string packer will be used to isolate the base of the hole so that pulse and flow tests can estimate hydrologic conditions, specifically the relation between bulk permeability and effective stress (e.g., Fisher et al., 1996).

## PROPOSED SITES

### Sites ACE-1c and ACE-7b

These proposed sites are situated near the southern limit of the coherently down-flexed northern margin, where the wedge of synrift sediments is thick and yet the seismic stratigraphy can be correlated easily over the margin to the north (Figs. 3-5). The stratal geometry, including two angular unconformities, requires that two sites be drilled to characterize this region.

Proposed Site ACE-1c is just north of a major south-dipping normal-fault system that is antithetic to the low-angle fault dipping north from Moresby Seamount (Fig. 4). It is also located above north-dipping reflectors at the base of the interpreted pre-rift forearc basin sequence. The expected sequence at Site ACE-1c includes 950 m of Quaternary hemipelagic, synrift sediments unconformably overlying 50 m of Paleogene volcanic or metamorphic basement.

Proposed Site ACE-7b is 15 km farther north on the margin and is positioned to cross two angular unconformities (Fig. 4). Beneath the lower angular unconformity a stratified sequence dips north. The expected section at Site ACE-7b includes 640 m of Pliocene-Quaternary hemipelagic sediments unconformably overlying 110 m of consolidated Miocene forearc basin sediments.

The primary objectives at these sites are to determine the (1) sedimentology, biostratigraphy, and vertical motion history of the northern margin; (2) nature of the forearc basin and basement sequence and hence the pre-rift history; and (3) in situ stress orientation, permeability, temperature, physical properties, and fluid composition in the basement for comparison with the same parameters in the active low-angle fault zone.

**Site ACE-3c**

This site is situated on a small bench just north of the crest of Moresby Seamount near where the basement reflector is shallowest (Figs. 3-5). The site is positioned in 420 m of water to avoid the possible safety and logistical constraints of shallower water drilling. However, 12-kHz records indicate the presence of only 6 m of ponded sediments above the northeast-dipping sediments seen on seismic records. Approximately 300 m of lithified sediments and 200 m of metamorphic basement may be drilled at this site.

The primary objective at this site is to determine the internal structure and composition of Moresby Seamount, including the nature of the basement (rock type, P-T-t, structural fabric, deformation history). By comparison with the stratigraphy and basement at the other sites, this will constrain the offset on the inferred low-angle normal fault. If Moresby Seamount is an upper plate fault block it should comprise sedimentary rocks above upper crustal rocks (presumably pre-rift metamorphic basement) without evidence of intense ductile deformation and rapid decompression.

**Site ACE-8a**

This proposed site is situated on the southern edge of the graben north of Moresby Seamount and will be drilled though the hanging wall, across the fault zone, and into the footwall of the inferred low-angle fault (Figs. 3-5). The expected section at Site ACE-8a includes up to 900 m of Quaternary hemipelagic sediments (only 0.7 seconds TWT, but apparently fast interval velocities averaging 2.6 km/s) overlying 300 m of fault zone and metamorphic basement rocks.

The primary objectives at this site are to determine the (1) sedimentology, biostratigraphy, structural fabric, and vertical motion history in the graben; (2) in situ stress, permeability, temperature, physical properties, and fluid pressures in and around the fault zone; and (3) nature of the basement (rock type, P-T-t, structural fabric, deformation history) in and below the fault zone.

**Site ACE-9a**

This is an alternate site between, and with the same objectives as, Sites ACE-1c and ACE-7b. It is also a potential operational compromise, if there is not enough time to drill both of these sites.

## REFERENCES

**Abers, G.A., 1991.** Possible seismogenic shallow-dipping normal faults in the Woodlark-D'Entrecasteaux extensional province, Papua New Guinea. *Geology*, 19:1205-1208.

**Abers, G.A., and Roecker, S.W., 1991.** Deep structure of an arc-continent collision: Earthquake relocation and inversion for upper mantle P and S wave velocities beneath Papua New Guinea. *J. Geophys. Res.*, 96:6379-6401.

**Abers, G.A., Mutter, C.Z., and Fang, J., in press.** Earthquakes and normal faults in the Woodlark-D'Entrecasteaux rift system, Papua New Guinea. *J. Geophys. Res.*.

**Ashley, P.M., and Flood, R.H., 1981.** Low-K tholeiites and high-K igneous rocks from Woodlark Island, Papua New Guinea. *J. Geol. Soc. Aust.*, 28:227-240.

**Axen, G.J., 1992.** Pore pressure, stress increase, and fault weakening in low-angle normal faulting. *J. Geophys. Res.*, 97:8979-8991.

**Baldwin, S.L., and Ireland, T.R., 1995.** A tale of two eras: Plio-Pleistocene unroofing of Cenozoic and late Archean zircons from active metamorphic core complexes, Solomon Sea, Papua New Guinea. *Geology*, 23:1023-1026.

**Baldwin, S.L., Lister, G.S., Hill, E.J., Foster, D.A., and McDougall, I., 1993.** Thermochronologic constraints on the tectonic evolution of active metamorphic core complexes, D'Entrecasteaux Islands, Papua New Guinea. *Tectonics*, 12:611-628.

**Barton, C.A., and Zoback, M.D., 1994.** Stress perturbations associated with active faults penetrated by boreholes; possible evidence for near-complete stress drop and a new technique for stress magnitude measurement. *J. Geophys. Res.*, 99:9373-9390.

**Barton, C.A., Zoback, M.D., and Moos, D., 1995.** Fluid flow along potentially active faults in crystalline rock. *Geology*, 23:683-686.

**Benes, V., Scott, S.D., and Binns, R.A., 1994.** Tectonics of rift propagation into a continental margin: western Woodlark Basin, Papua New Guinea. *J. Geophys. Res.*, 99:4439-4455.

**Binns, R.A., Scott, S.D., et al., 1987.** Western Woodlark Basin: Potential analogue setting for volcanogenic massive sulphide deposits. *Proc. Pacific Rim Congr.*, 87:531-535.

**Binns, R.A., Scott, S.D. et al., 1989.** *Propagation of sea-floor spreading into continental crust, western Woodlark Basin, Papua New Guinea*, CCOP/SOPAC Misc. Rept.

**Binns, R.A., Scott, S.D., Wheller, G.E., and Benes, V., 1990.** *Report on the SUPACLARK cruise, Woodlark Basin, Papua New Guinea, April 8-28 1990, RV Akademik Mstislav Keldysh*. CSIRO Rept. 176R.

**Binns, R.A., and Whitford, D.J., 1987.** Volcanic rocks from the western Woodlark Basin, Papua New Guinea. *Proc. Pacific Rim Congress*, 87:525-534.

**Davies, H.L., 1980.** Folded thrust and associated metamorphics in the Suckling-Dayman massif, Papua New Guinea. *Am. J. Sci.*, 280:171-191.

**Davies, H.L., and Jaques, A.L., 1984.** Emplacement of ophiolite in Papua New Guinea. *Spec. Publ. Geol. Soc. Lond.*, 13:341-350.

**Davies, H.L., and Smith, I.E., 1971.** Geology of eastern Papua. *Geol. Soc. Am. Bull.*, 82:3299-3312.

**Davies, H.L., Symonds, P.A., and Ripper, I.D., 1984.** Structure and evolution of the southern Solomon Sea region. *BMR J. Aust. Geol. Geophys.*, 9:49-68.

**Davies, H.L., and Warren, R.G., 1988.** Origin of eclogite-bearing, domed, layered metamorphic complexes ("core complexes") in the D'Entrecasteaux Islands, Papua New Guinea. *Tectonics*, 7:1-21.

**Davies, H.L., and Warren, R.G., 1992.** Eclogites of the D'Entrecasteaux Islands. *Contrib. Mineral. Petrol.*, 112:463-474.

**Finlayson, D.M., Muirhead, K.J., Webb, J.B., Gibson, G., Furumoto, A.S., Cooke, R.J.S., and Russel, A.J., 1976.** Seismic investigation of the Papuan Ultramafic Belt. *Geophys. J. R. Astron. Soc.*, 29:245-253.

**Fisher, A.T., Zwart, G., and ODP Leg 156 Scientific Party, 1996.** Relation between permeability and effective stress along a plate-boundary fault, Barbados accretionary complex. *Geology*, 24:307-310.

**Francis, G., Lock, J., and Okuda, Y., 1987.** Seismic stratigraphy and structure of the area to the southeast of the Trobriand Platform. *Geo-Marine Lett.*, 7:121-128.

**Gill, J.B., Morris, J.D., and Johnson, R.W., 1993.** Time scale for producing the geochemical signature of island arc magmas: U-Th-Po and Be-B systematics in recent Papua New Guinea lavas. *Geochim. Cosmochim. Acta*, 57:4269-4283.

**Goodliffe, A., Taylor, B., Hey, R., and Martinez, F., 1993.** Seismic images of continental breakup in the Woodlark Basin, PNG. *Eos, Trans. AGU*, 74:606.

**Goodliffe, A., Taylor, B., Martinez, F., Hey, R., Maeda, K., and Ohno, K., 1997.** Synchronous reorientation of the Woodlark Basin spreading center. *Earth Planet. Sci. Lett.*, 146:233-242.

**Hamilton, W., 1979.** Tectonics of the Indonesian region, *U.S. Geol. Surv. Prof. Paper,* 1078.

**Hegner, E., and Smith, I.E.M., 1992.** Isotopic compositions of late Cenozoic volcanics from southeast Papua New Guinea: evidence for multi-component sources in arc and rift environments. *Chem. Geol.*, 97:233-249.

**Hickman, S., Sibson, R., and Bruhn, R. (Eds.), 1993.** Proceedings of Workshop LXIII: The Mechanical Involvement of Fluids in Faulting. *U.S. Geol. Surv. Open File Rpt.*, 94-228.

**Hill, E.J., 1987.** Active extension in the D'Entrecasteaux Islands, Papua New Guinea. *BMR Res. Symp.,* 87:51-57.

**Hill, E.J., 1990.** The nature of shear zones formed during extension in eastern Papua New Guinea. *Proc. Pacific Rim Congr.*, 90:537-548.

**Hill, E.J., 1994.** Geometry and kinematics of shear zones formed during continental extension in eastern Papua New Guinea. *J. Structural Geol.*, 16:1093-1105,.

**Hill, E.J., 1995.** Extensional deformation of continental crust prior to break-up and sea-floor spreading: a study of Misima Island, Papua New Guinea. *Geol Soc. Aust. Abstr.* 9.

**Hill, E.J., and Baldwin, S.L, 1993.** Exhumation of high-pressure metamorphic rocks during crustal extension in the D'Entrecasteaux region: Papua New Guinea. *J. Metamorphic Geol.*, 11:261-277.

**Hill, E.J., Baldwin, S.L., and Lister, G.S., 1992.** Unroofing of active metamorphic core complexes in the D'Entrecasteaux Islands, Papua New Guinea. *Geology*, 20:907-910.

**Hill, E.J., Baldwin, S.L., and Lister, G.S., 1995.** Magmatism as an essential driving force for formation of active metamorphic core complexes in eastern Papua New Guinea. *J. Geophys. Res.*, 100:10,441-10,451.

**Lisitsin, A.P., and 8 others, 1991.** Present-day hydrothermal activity at Franklin Seamount, western Woodlark Sea (Papua New Guinea). *Internat. Geol. Rev.*, 33:914-929.

**Lister, G.S., and Baldwin, S.L., 1993.** Plutonism and the origin of metamorphic core complexes. *Geology,* 21:607-610.

**Lock, J., Davies, H.L., Tiffin, D.L., Murakami, F., and Kisomoto, K., 1987.** The Trobriand Subduction system in the Western Solomon Sea. *Geomarine Lett.,* 7:129-134.

**Mutter, J.C., Mutter, C.Z., Abers, G., and Fang, J., 1993.** Seismic images of low-angle normal faults in the western Woodlark Basin where continental extension yields to seafloor spreading. *Eos, Trans. AGU,* 74:412.

**Mutter, J.C., Mutter, C.Z., and Fang, J., 1996.** Analogies to oceanic behaviour in the continental breakup of the western Woodlark Basin. *Nature,* 380:333-336.

**Pinchin, J., and Bembrick, C., 1985.** Cape Vogel Basin, PNG - tectonics and petroleum potential. *In 14th BMR Symposium Extended Abstracts: Petroleum Geology of South Pacific Island Countries.* Bur. Min. Resour. Aust. Rec., 32:31-37.

**Rice, J.R., 1992.** Fault stress states, pore pressure distributions, and the weakness of the San Andreas fault, *In* Evans, B., and Wong, T.-F. (Eds.), *Fault Mechanics and Transport Properties of Rock (Int. Geophys. Ser. 51),* Academic Press.

**Rogerson, R., Hilyard, D., Francis, G., and Finlayson, E., 1987.** The foreland thrust belt of Papua New Guinea. *Proc. Pacific Rim Congress,* 87:579-583.

**Rogerson, R., Queen, L., and Francis, G., 1993.** The Papuan Ultramafic Belt Arc Complex, *In* Wheller, G. E. (Ed.), *Islands and Basins: Correlation and Comparison of Onshore and Offshore Geology.* CCOP/SOPAC Misc. Rept. 159:28-29.

**Smith, I.E., and Simpson, C.J., 1972.** Late Cenozoic uplift in the Milne Bay area, eastern Papua New Guinea. *Bur. Min. Resour. Aust. Bull.*, 125:29-35.

**Smith, I.E.M., 1976.** Peralkaline rhyolites from the D'Entrecasteaux Islands, Papua New Guinea, *In* Johnson, R.W. (Ed.), *Volcanism in Australasia*: Amsterdam (Elsevier), 275-285.

**Smith, I.E.M., and Milsom, J.S., 1984.** Late Cenozoic volcanism and extension in eastern Papua. *In*

Kokelaar, B.P., and Howells, M.F. (Eds.), *Marginal Basin Geology*, Geol. Soc. Spec. Publ., 16:163-171.

**Stewart, W.P., Francis, G., and Deibert, D.H., 1986.** Hydrocarbon potential of the Cape Vogel Basin, Papua New Guinea. *Geol. Surv. Papua New Guinea Rept. No. 86/10*.

**Stolz, A.J., Davies, G.R., Crawford, A.J., and Smith, I.E.M., 1993.** Sr, Nd and Pb isotopic compositions of Calc-alkaline and peralkaline silicic volcanics from the D'Entrecasteaux Islands, Papua New Guinea, and their tectonic significance. *Mineral. and Petrol*, 47:103-126.

**Taylor, B., 1987.** A geophysical survey of the Woodlark-Solomons region. *In* Taylor, B. and Exon, N.F., (Eds.), *Marine Geology, Geophysics and Geochemistry of the Woodlark Basin - Solomon Islands*, Earth Science Series, 7: (Circum-Pacific Council for Energy and Mineral Resources) Houston, Tx, 25-48.

**Taylor, B., and Exon, N.F., 1987.** An investigation of ridge subduction in the Woodlark-Solomons region: Introduction and overview. *In* Taylor, B. and Exon, N.F., (Eds.), *Marine Geology, Geophysics and Geochemistry of the Woodlark Basin - Solomon Islands*, Earth Science Series, 7: (Circum-Pacific Council for Energy and Mineral Resources) Houston, Tx, 1-24.

**Taylor, B., Goodliffe, A., Martinez, F., and Hey, R., 1995.** A new view of continental rifting and initial seafloor spreading. *Nature*, 374:534-537.

**Taylor, B., Mutter, C., Goodliffe, A., and Fang, J., 1996.** Active continental extension: the Woodlark Basin, *JOI/USSAC Newsletter*, 9:1-4.

**Tjhin, K.T., 1976.** Trobriand Basin Exploration, Papua New Guinea. *The APEA J.*, 81-90.

**Walker, D.A., and McDougall, I., 1982.** $^{40}$Ar/$^{39}$Ar and K-Ar dating of altered glassy volcanic rocks: the Dabi Volcanics, P.N.G. *Geochim. Cosmochim. Acta*, 46:2181-2190.

**Weissel, J.K., Taylor, B., and Karner, G.D., 1982.** The opening of the Woodlark Basin, subduction of the Woodlark spreading system and the evolution of northern Melanesia since mid-Pliocene time. *Tectonophysics*, 87:253-277.

**Wernicke, B., 1995.** Low-angle normal faults and seismicity: a review, *J. Geophys. Res.*, 100:20159-20174.

**Worthing, M.A., 1988.** Petrology and tectonic setting of blueschist facies metabasites from the Emo Metamorphics of Papua New Guinea. *Aust. J. Earth Sci.*, 35:159-168.

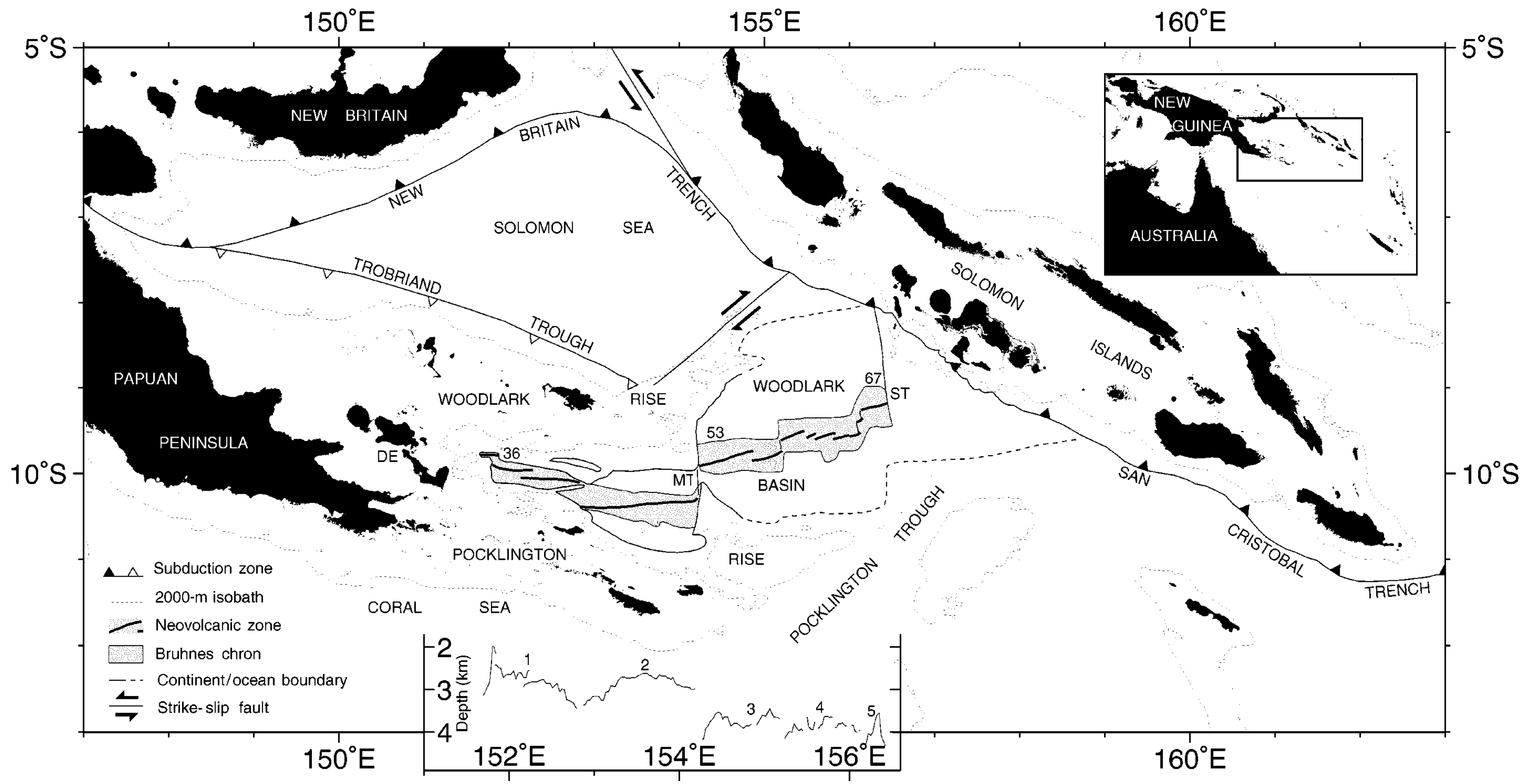


FIG. 1 Major physiographic features and active plate boundaries of the Woodlark basin region. The stippled area encloses oceanic crust formed during the Brunhes chron at spreading rates labelled in mm/yr. MT and ST, Moresby and Simbo transform faults, respectively; DE, D'Entrecasteaux islands. Top inset, geographial location of the Woodlark basin. Bottom inset, depth profile along the axis of the spreading center, with the five spreading segments numbered.

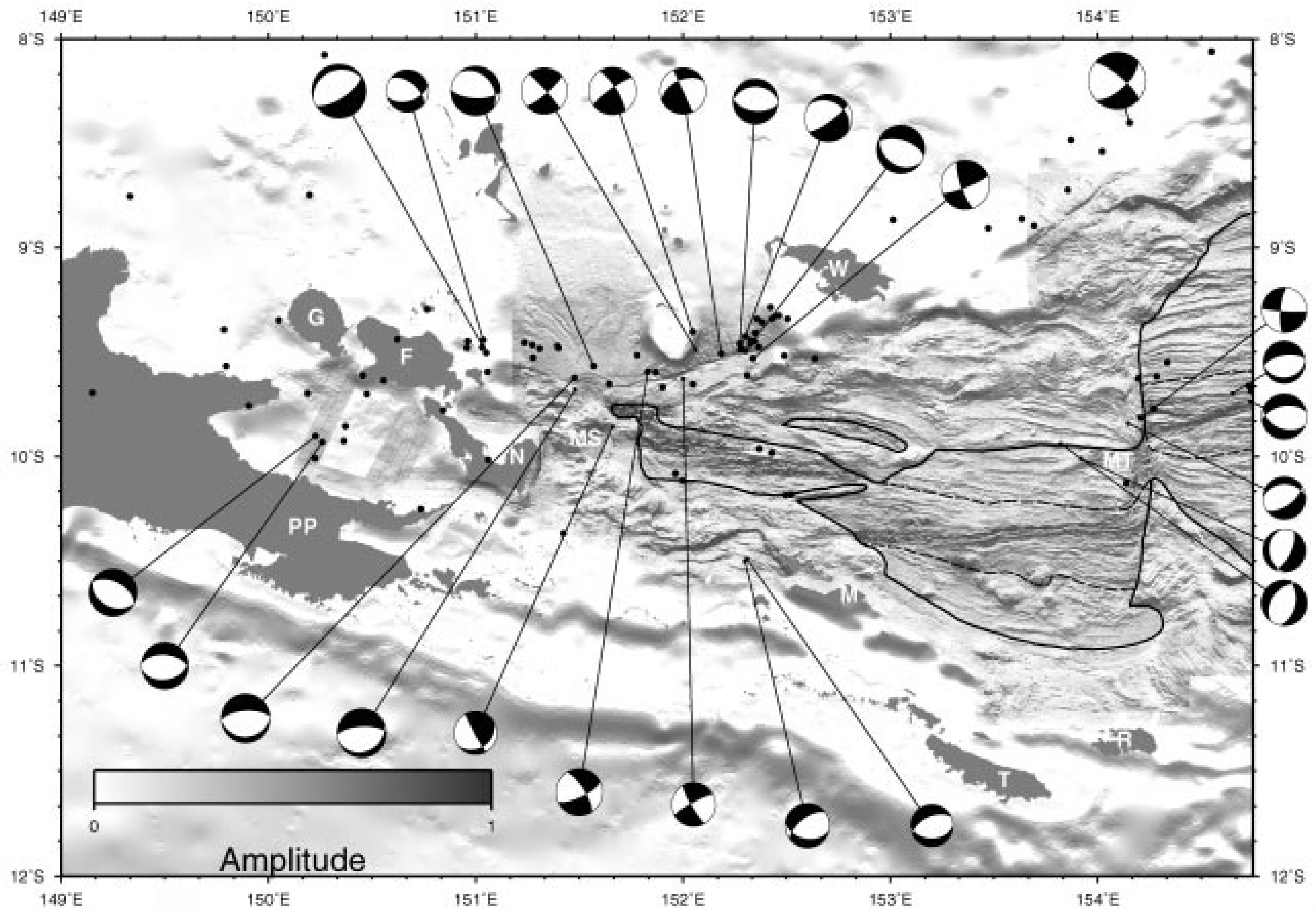


FIG. 2 HAWAII MR1 bathymetric texture and acoustic imagery. Relocated epicenters (black circles) and earthquake focal mechanisms are from Abers et al (1997). PP, Papuan peninsula; G, Goodenough island; F, Fergusson island; N, Normanby island; R, Rossel island; T, Tagula island; MS, Moresby seamount; MT, Moresby transform fault; M, Misima island; W, Woodlark island. The solid line is the landward boundary of oceanic crust, and the dashed line marks the boundary of crust formed during the Brunhes chron.

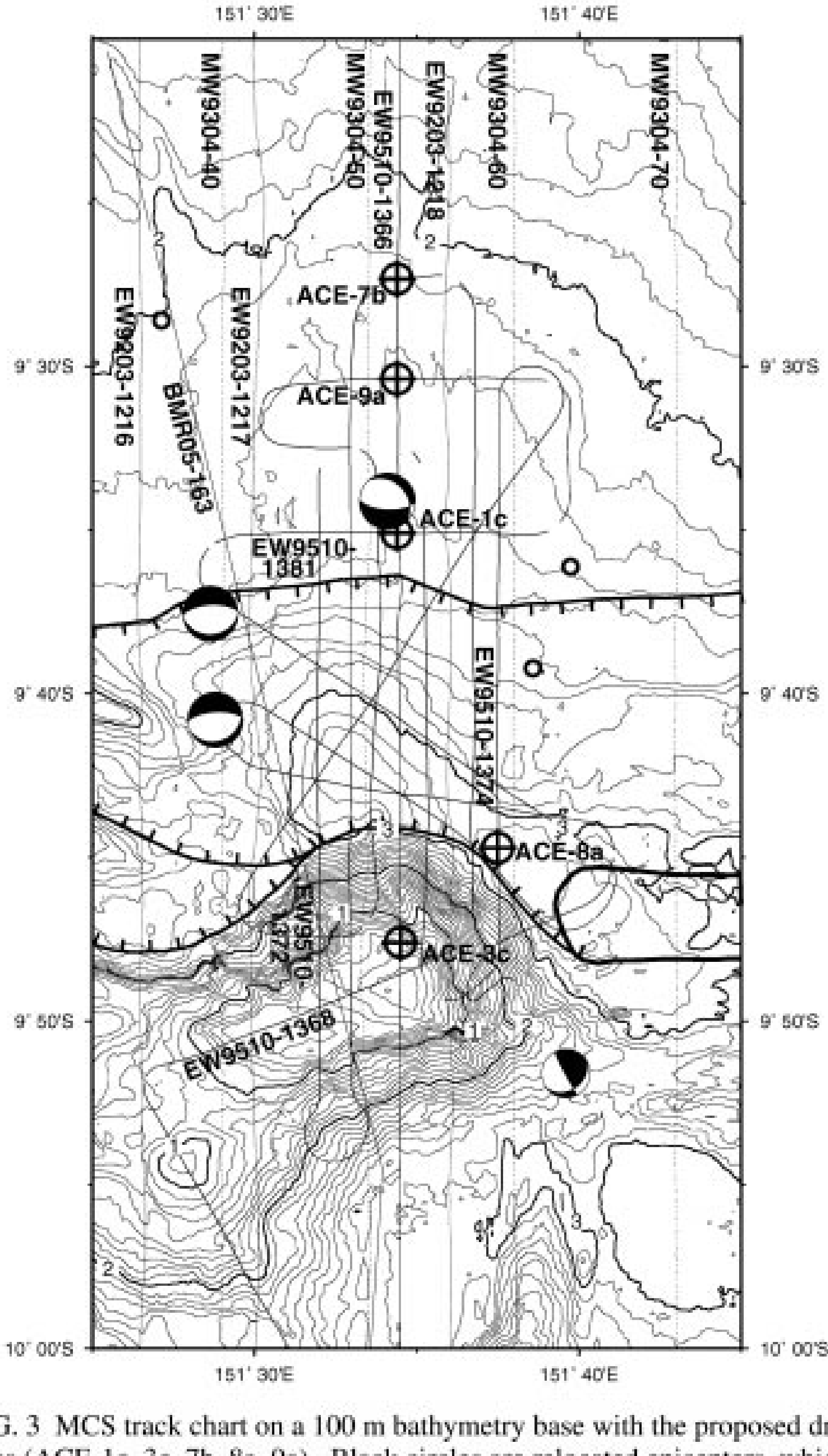


FIG. 3 MCS track chart on a 100 m bathymetry base with the proposed drill sites (ACE-1c, 3c, 7b, 8a, 9a). Black circles are relocated epicenters, which together with the focal mechanisms, are from Abers et al (1997). The western limit of the Woodlark spreading system is marked by the closed black line, major normal faults by the ticked lines.

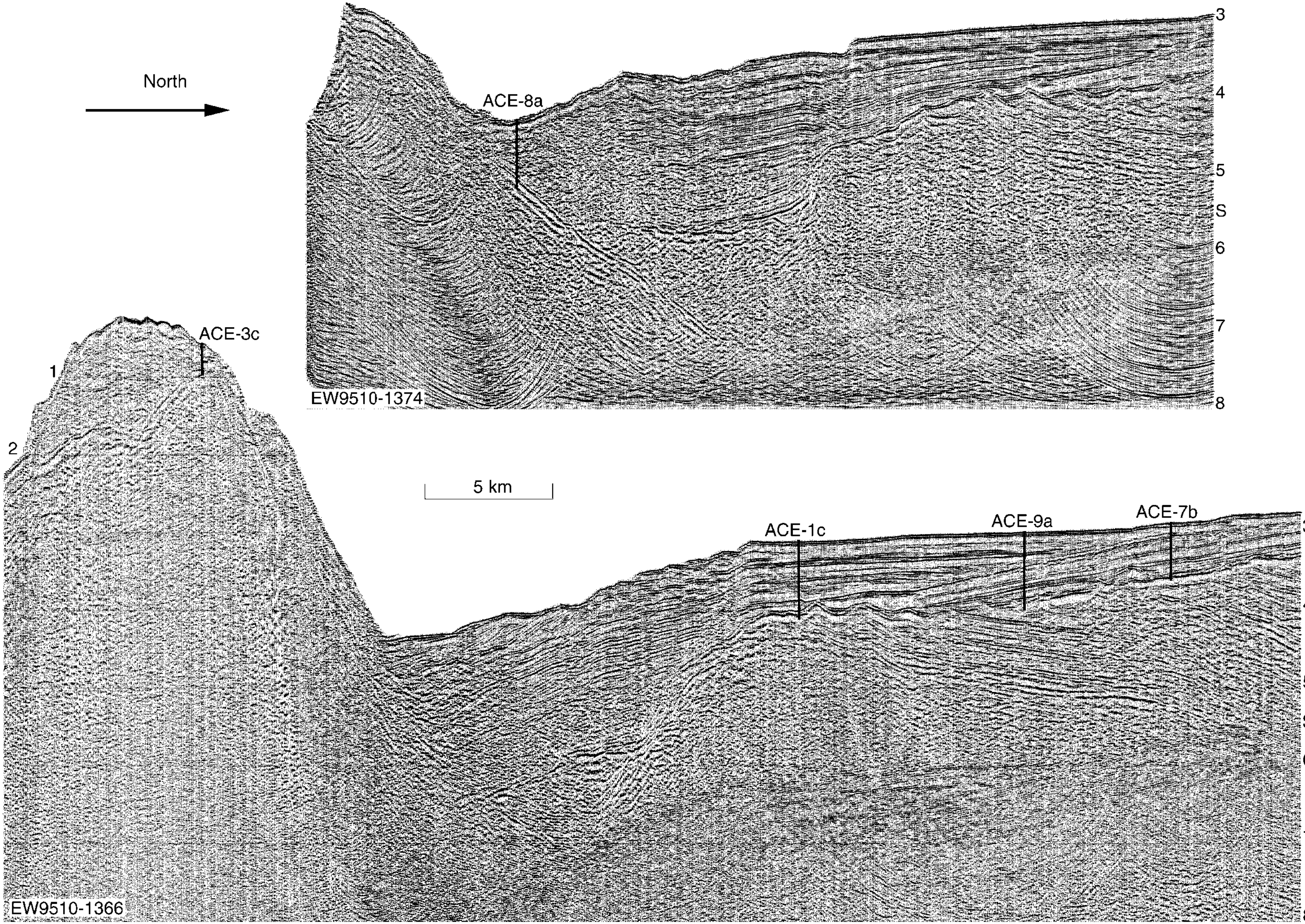


FIG. 4 Migrated seismic profiles showing the location of the proposed drill sites ACE-1c, 3c, 7b, 8a and 9a.

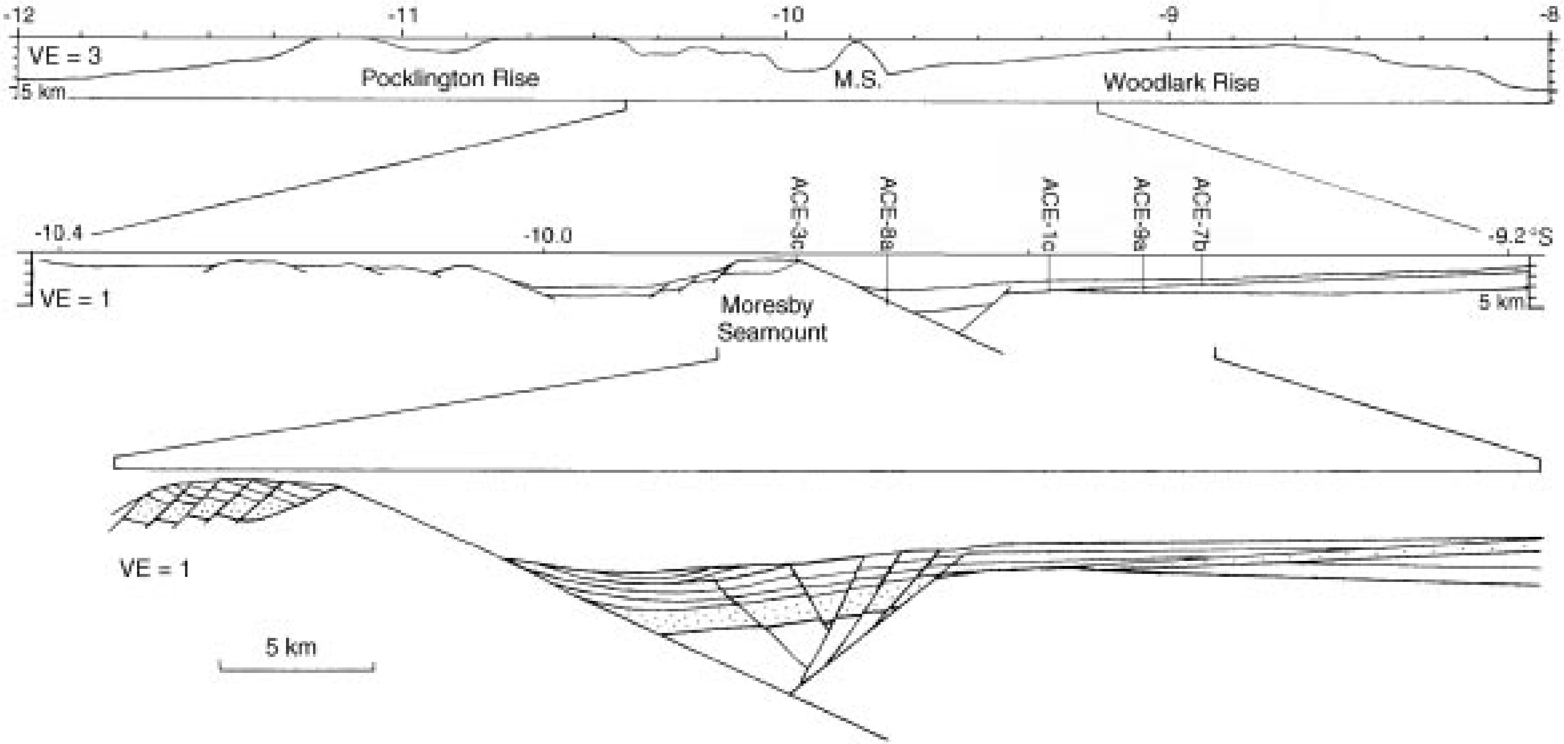


FIG. 5 Nested meridional sections showing the regional and local structures across the incipient conjugate margins. The proposed drill sites are ACE-1c, 3c, 7b, 8a and 9a.

# TABLE 1

## PROPOSED SITE INFORMATION AND DRILLING STRATEGY

| | | |
|---|---|---|
| **SITE**: ACE-1c | **PRIORITY**: 1 | **POSITION**: 9°35.117'S, 151°34.424'E |
| **WATER DEPTH**: 2307 m | **SEDIMENT THICKNESS**: 950 m | **TOTAL PENETRATION**: 1030 m |
| **SEISMIC COVERAGE:** EW9510-1366 (WW01 CMP 4547) and -1381 (WW13 CMP 1681) | | |

**Objectives**: Determine (1) sedimentology, biostratigraphy, and vertical motion history of the northern margin; (2) nature of basement and the pre-rift history; and (3) basement stress orientation, permeability, temperature, physical properties, and fluid composition.

**Drilling Program**: APC, XCB, RCB.

**Logging and Downhole Operations**: Triple-combo, FMS, GHMT, BHTV in basement.

**Nature of Rock Anticipated**: Quaternary hemipelagic sediments, Paleogene volcanics and volcaniclastics.

| | | |
|---|---|---|
| **SITE**: ACE-3c | **PRIORITY**: 1 | **POSITION**: 9°47.61'S, 151°34.50'E |
| **WATER DEPTH**: 420 m | **SEDIMENT THICKNESS**: 300 m | **TOTAL PENETRATION**: 500 m |
| **SEISMIC COVERAGE**: EW9510-1366 (WW01 CMP 6390) | | |

**Objectives**: Determine internal structure and composition of Moresby Seamount including the nature of basement (rock type, P-T-t, structural fabric, and deformation history).

**Drilling Program**: APC, XCB, RCB.

**Logging and Downhole Operations**: Triple-combo, FMS, GHMT, BHTV in basement.

**Nature of Rock Anticipated**: 6 m Holocene carbonate sand; Quaternary sandstone, siltstone and mudstone; greenschist facies metamorphics.

| | | |
|---|---|---|
| **SITE**: ACE-7b | **PRIORITY**: 1 | **POSITION**: 9°27.327'S, 151°34.396'E |
| **WATER DEPTH**: 2115 m | **SEDIMENT THICKNESS**: 750 m | **TOTAL PENETRATION**: 750 m |
| **SEISMIC COVERAGE:** EW9510-1366 (WW01 CMP 3399) and -1370 (WW4a CMP 1208) | | |

**Objectives**: Determine (1) sedimentology, biostratigraphy, and vertical motion history of the northern margin, and (2) nature of the forearc basin sequence and the pre-rift history.

**Drilling Program**: APC, XCB, RCB.

**Logging and Downhole Operations**: Triple-combo, FMS, GHMT.

**Nature of Rock Anticipated**: 640 m Pliocene-Quaternary hemipelagic sediments above 110 m Miocene forearc basin sediments (sandstone, siltstone, and mudstone).

| | | |
|---|---|---|
| **SITE**: ACE-8a | **PRIORITY**: 1 | **POSITION**: 9°44.71'S, 151°37.52'E |
| **WATER DEPTH**: 3175 m | **SEDIMENT THICKNESS**: 900 m | **TOTAL PENETRATION**: 1200 m |
| **SEISMIC COVERAGE**: EW9510-1374 (WW08 CMP 1500) | | |

**Objectives**: Determine (1) sedimentology, biostratigraphy, structural fabric and vertical motion history in the rift graben, (2) nature of basement (P-T-t, structural fabric, deformation history) in and below fault zone, and (3) in situ stress, permeability, temperature, physical properties, fluid pressure, and composition.

**Drilling Program**: APC, XCB, RCB, Reentry and triple casing.

**Logging and Downhole Operations**: Triple-combo, FMS, GHMT, BHTV in basement, ASI VSP, packer experiments.

**Nature of Rock Anticipated**: Quaternary hemipelagic sediments, sheared fault zone rocks, metamorphics.

| | | |
|---|---|---|
| **SITE**: ACE-9a | **PRIORITY**: 2 | **POSITION**: 9°30.387'S, 151°34.393'E |
| **WATER DEPTH**: 2211 m | **SEDIMENT THICKNESS**: 1000 m | **TOTAL PENETRATION**: 1000 |
| **SEISMIC COVERAGE**: EW9510-1366 (WW01 CMP 3850) & -1379 (WW11 CMP 1624) | | |

**Objectives**: Determine (1) sedimentology, biostratigraphy, and vertical motion history of the northern margin, (2) nature of the forearc basin sequence and the pre-rift history.

**Drilling Program**: APC, XCB, RCB.

**Logging and Downhole Operations**: Triple-combo, FMS, GHMT.

**Nature of Rock Anticipated**: 780 m Pliocene-Quaternary hemipelagic sediments above 220 m Miocene forearc basin sediments (sandstone, siltstone, and mudstone).